Asynchronous Cooperative Transmission in Underwater Acoustic Networks

Ping Wang*, Wei Feng*, Lin Zhang* and Victor O.K. Li**
*Department of Electronic Engineering, Tsinghua University, Beijing, China
**Dep. of Electrical & Electronic Engineering, University of Hong Kong, Hong Kong, China
Email: ping-wang07@mails.tsinghua.edu.cn, feng_wei@mail.tsinghua.edu.cn
linzhang@tsinghua.edu.cn, vli@eee.hku.hk

***Abstract*—Multi-path fading, one of the key factors that deteriorate quality of service (QOS) in Underwater Acoustic Networks (UANs), is investigated under different underwater scenarios in this paper. To improve the Bit Error Rate (BER) performance, the techniques of cooperative diversities are applied. Considering realistic physical model and cooperative diversity techniques, two asynchronous forwarding schemes, namely Underwater Amplify-and-Forward (UAF) and Underwater Decode-and-Forward (UDF), are proposed and analyzed. The results show that both UDF and UAF have better performance than direct transmission. Furthermore, an adaptive and hybrid forwarding scheme is proposed based on UAF and UDF.**

***Keywords*-Underwater Acoustic Networks, Amplify-and-Forward, Decode-and-Forward, Hybrid Forwarding Scheme**

I. Introduction

In recent years, Underwater Acoustic Networks (UANs) have attracted growing interests [1], [2]. Firstly, it is motivated by various aquatic applications, such as mineral exploitation, environmental monitoring, disaster prevention, military surveillance and coastline protection. Secondly, communication in aquatic environments is characterized by large propagation delay, limited bandwidth, and high and complex noise [1], rendering technologies designed for terrestrial radio communication and networking not applicable for UANs and imposing new challenges.

In UANs, the channel quality is dominated by the complex underwater scenarios, especially the path loss caused by multi-path fading [6]. Path loss is dependent on both the communication range and carrier frequency, and it increases quickly as carrier frequency increases [2]. To alleviate the effects of fading, frequency and spatial diversity are the basic diversity techniques. In additional to these traditional diversity techniques, cooperative transmission may be used.

Transmission cooperative diversity is first applied in underwater networks in [5] and [6], and recent research has shown that the performance of UANs can be greatly improved by employing transmission cooperative diversity [5], [6], [7], [8], [9]. In [5], multi-hop cooperation schemes for underwater sensor networks are studied and it is shown to be highly energy efficient. In this work, the Decode-and-Forward strategy (where the relay node decodes, re-encodes and forwards the signal received from its immediate predecessor in the network) is considered. In [6], protocols coupled with Space-Time Block Code (STBC) strategies are proposed and analyzed for distributed cooperation communication, where Amplify-and-forward-type protocols (where the relay node amplifies and forwards the signal received from its immediate predecessor in the network) are adopted. Similarly, in [7], Amplify-and-Forward scheme is utilized in UANs, and the simulation results show that the quality of image transmissions is improved. In [8], the author studied the differences between direct transmission and cooperative transmission, and proposed a new cooperation transmission scheme for the underwater environment, mainly focusing on improving channel capacity. In [9], cooperative transmission has been proved to be an energy efficient solution for time-varying multi-path fading underwater channel. To summarise, these studies prove that cooperative transmission can improve channel capacity and data reliability for UANs.

To the best of our knowledge, only synchronous cooperative transmission techniques have been considered in previous work of UANs. However, large and variable propagation delay in underwater acoustic communication that is five orders larger than that in wireless radio networks, makes implementation of synchronous cooperative transmission in UANs difficult and cost. Therefore, in this paper, asynchronous cooperative transmission techniques will be used. Furthermore, two typical diversity techniques, Amplify-and-Forward (AF) and Decode-and-Forward (DF), are implemented in UANs to improve the network performance.

The remainder of the paper is organized as follows. Section II introduces necessary preliminaries, including underwater channel model and system model with three terminals. In Section III, asynchronous cooperative transmissions are designed for UANs. Performances of UAF, UDF, and direct transmission are theoretically analyzed and compared in Section IV. Besides, an adaptively forwarding scheme is described in Section IV. The simulation results are given in Section V. Finally, we conclude and suggest future research directions.

II. Preliminaries

A. Underwater Sound Channel Model

Similar to [10], [11], [13], [14], a ray-based model is used to model the multipath sound propagation with a channel impulse

response $h(t,\tau)$ as shown in (1).

$$h(t,\tau) = \sum_{i=1}^{p} h_i(t)\delta(t-\tau_i) \tag{1}$$

where *p* is the number of macro-paths, $h_i(t)$ is the *i-th* channel coefficient, and τ_i is the delay spread for the *i-th* path. These parameters are based on propagation of sound wave in water. The Bellhop model which implements the method of Gaussian beam tracing [15] is utilized to compute these parameters.

The speed of sound depends on three factors: water salinity, temperature, and density. The speed increases with the increse of any one of the above three factors. Several empirical formulae have been proposed by oceanographists. Here we present Coppens equation as an example (refer to [16] for coefficient values). Coppens equation for sound speed is in meters/second.

$$\begin{aligned} C_{D_e,S_a,T_e} = c_0 + c_1T_e + c_2T_e^2 + (c_4 + c_5T_e + c_6T_e^2)(S_a - 35) \\ +(c_7 + c_8T_e)D_e + (c_9 + c_{10}T_e)D_e^2 \\ +[c_{11} + c_{12}(S_a - 35)](S_a - 35)T_eD_e \end{aligned} \tag{2}$$

where D_e is the depth in meters, S_a is salinity in parts per thousand (ppt), and T_e is water temperature in degrees Celsius.

Basically, according to different sound speed profiles, four representative types of distributions for sound speed are considered in this work, including constant speed, negative gradient, positive gradient, and layered. The sound-speed profiles and ray-based sound channel are illustrated in Fig. 1(a), (b), (c), and (d), where C_w is the sound speed in water in meters/second, ρ_w is water density in gramme/cubic centimeter, C_b is sound speed in the bottom medium in meters/second, ρ_b is density of bottom medium in gramme/cubic centimeter and α_b is attenuation coefficient in bottom medium in dB/wavelength [12].

Due to non-uniformity of the water medium, the sound path will bend towards the medium with smaller sound speed. Based on the Bellhop model, we can obtain the channel impulse response function for the abovementioned four types of sound speed distribution, with both the source node and the destination node located 10 meters underwater and 2000 meters apart, as in Fig. 2 (a), (b), (c) and (d). We can find that multipath propagation in shallow water channel (eg. Fig. 2 (a), (b) and (c))is more severe than that in deep water channel. In Section IV we will simulate to compare the performances of different cooperation strategies with these different sound speed profiles.

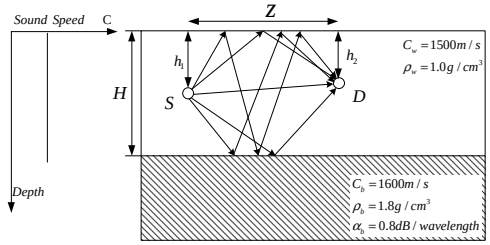

(a) Constant Sound Speed

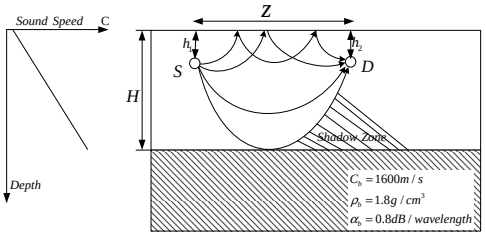

(b) Sound Speed with Positive Gradient

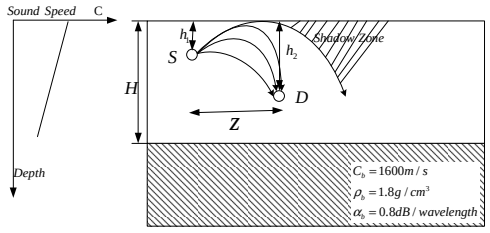

(c) Sound Speed with Negative Gradient

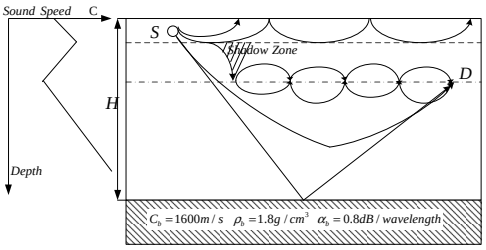

(d) Layered Sound Speed

Fig. 1. Soundspeed Profile and Ray Diagram-based Sound Channel

B. System Model

As shown in Fig. 3, our system model consists of three nodes: a source node (*S*), a relay node (*R*) and a destination node (*D*). The sea depth is *H* meters. The source node, the relay node, and the destination node are located underwater, respectively, at h_1, h_2, and h_3 meters. The horizontal ranges between S and R, R and D, S and D are z_1, z_2, and z_3 meters, respectively. This system model can be regarded as a basic component of multi-hop cooperation scenarios. By studying it thoroughly, we can get valuable insights into more realistic scenarios such as multi-hop cooperation scenario and multi-path cooperation scenario. In this work, we have the following assumptions:

1) All the links are independent and modeled as Nakagami-m[1] distribution fading channel, and the parameter is computed by the Bellhop model.
2) Two stages are required to complete one packet transmission: (a) Relay receiving stage : The source node transmits, the relay and the destination receive; (b) Relay transmitting stage: The relay transmits, the destination receives.
3) The power at the transmitter and relay are limited, at P_S and P_R, respectively.
4) Let T_s be a symbol duration and τ_{ki} be delays for

[1]The Nakagami-m distribution can model a range of fading channels from one-sided Gaussian fading ($m = 1/2$, worst-case fading) to nonfading ($m =$). $m = 1$ is a special case, equivalent to Rayleigh fading [20]. Some papers state that the Rician distribution can be closely approximated by the Nakagami-m distribution when $m > 1$. In [21], Nakagami-m distribution is found to be the closest match to underwater channel.

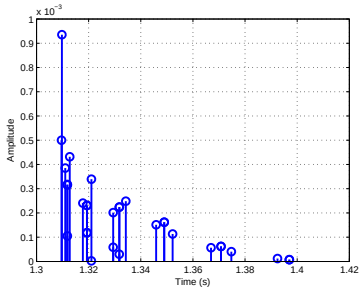

(a) Sea Depth 62 m, Constant Sound Speed

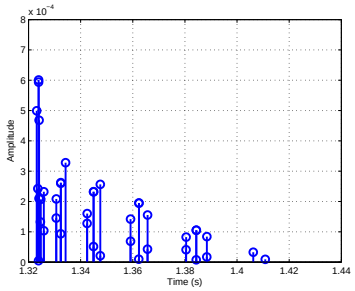

(b) Sea Depth 62m, Sound Speed with Positive Gradient

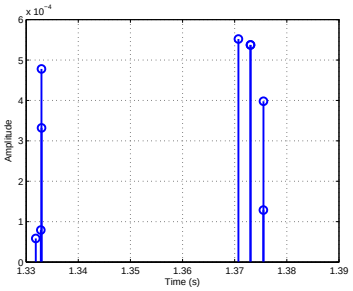

(c) Sea Depth 216 m, Sound Speed with Negative Gradient

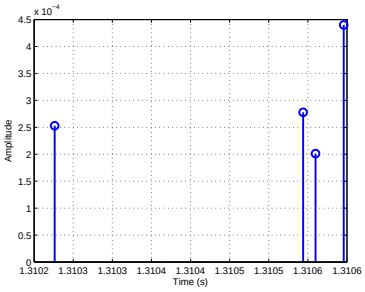

(d) Sea Depth 5000 m, Layered Sound Speed

Fig. 2. Channel Amplitude-Delay Profiles under Different Environments

signals along path k to arrive at the receiving node i, then we allow for $\tau_{ki} \leq T_s$, for any eigen-path $k, k \in 1, 2, ..., p$. Therefore, inter-symbol interference can be neglected.

5) The channel distribution information (CDI) is known at both the transmitter and the receiver, while the channel state information (CSI) is known at the receiver only.

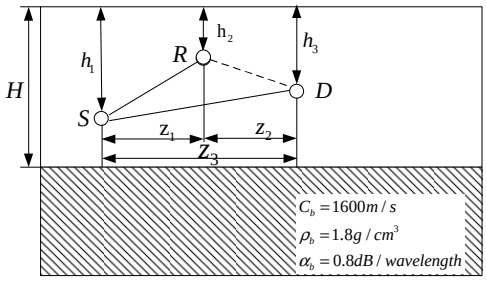

Fig. 3. System Model

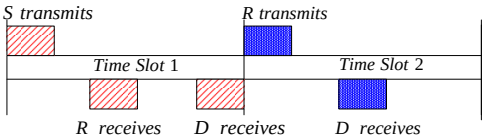

Fig. 4. Two-Stage Packet Transmission with AF/DF

III. Cooperation in UANs

A. Traditional Cooperation Schemes and Drawbacks in Underwater Environments

Cooperative transmission is a new wireless communication technique in which diversity gain is achieved by utilizing relay nodes as virtual antennas. Although the noise of the relay node is amplified with Amplify-and-Forward and there may be some error propagation in Decode-and-Forward, the destination node still receives signals that experience independent fading and is thus able to make better decisions on the transmitted signals.

Traditionally, transmission cooperative diversity in wireless radio networks are implemented in time or frequency division channels.

However, as introduced in Section II, underwater channel has large and variable propagation delays (which are five orders larger than that in wireless electromagnetic communication), time synchronization among sensor nodes in UANs is quite costly and difficult. Besides, the length of each time slot that is required to accommodate the maximum link propagation delay will make channel efficiency quite low.

To clearly explain the impacts of propagation delay, an example is shown in Fig. 4, where cooperative transmission is implemented in two time slots. In time slot 1, the data packet is transmitted by the source node to the relay and the destination nodes respectively. In time slot 2, the packet received by the relay node is sent to the destination node. If the maximal distance among three links, including $S \rightarrow R$ link, $R \rightarrow D$ link, and $S \rightarrow D$ link, is 3 kilometers, the sound speed is 1500 meters per second, the packet size is 250 Bytes, and the bandwidth is 5 kHz, the length for each time slot should be not less than 2.4 ($\frac{250\times 8}{5\times 10^3} + \frac{3000}{1500} = 2.4$) seconds. Such long time slot will badly decrease the channel capacity.

Moreover, the frequency resources are badly limited in UANs, therefore, frequency division is not efficient here. To relieve the impacts of propagation delay, in this paper we propose asynchronous cooperation diversities for UANs.

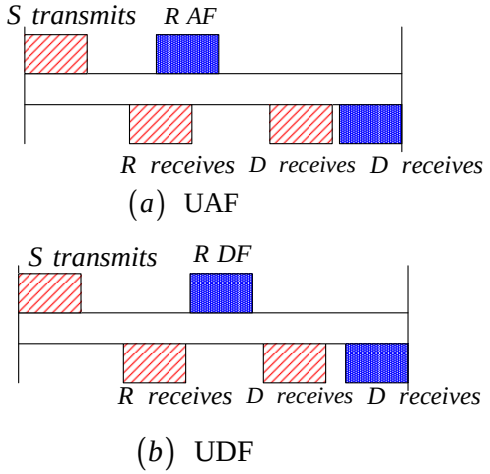

Fig. 5. Asynchronous transmission cooperative diversity in UANs

B. Asynchronous Cooperation in UANs

According to the unique characteristics of underwater acoustic channel, we propose an asynchronous cooperative transmission scheme, in which the relay node simply processes the signals received from the source and retransmits it to the destination immediately, instead of retransmitting in the next time slot.

Based on the two basic modes of signal processing techniques, Amplifying-and-Forward and Decode-and-Forward, we implement them in asynchronous manners as shown in Fig. 5 (a) and (b), and proposed Underwater Amplify-and-Forward (UAF) and Underwater Decode-and-Forward (UDF), suited for underwater communications.

IV. Performance Analysis

In the following subsections, the Bit Error Rate performance of transmission cooperative diversity with UAF, UDF, and direct transmission scheme are analyzed and compared.

A. UAF Mode

As shown in Fig. 5 (a), in proposed UAF cooperation transmission scheme, the relay node simply amplifies the signal received from the source and forwards it to the destination immediately, instead of transmitting in the next time slot.

In our UANs model, the signals received at the relay and the destination can be written as (3) and (4), respectively.

$$Y_{SR} = \sqrt{P_S} h_{SR} X_S + n_{SR} \tag{3}$$

$$Y_{SD} = \sqrt{P_S} h_{SD} X_S + n_{SD} \tag{4}$$

where P_S is the signal transmission power, X_S is a transmitted signal with unit energy, h_{SR}, which has the form of (1), denotes the channel gain for the $S \rightarrow R$ channel, h_{SD} is the channel gain for the $S \rightarrow D$ channel, n_{SR} and n_{SD}, are additive gaussian noises with zero mean and variance σ^2 for the $S \rightarrow R$ channel and the $S \rightarrow D$ channel, respectively.

The relay node amplifies the received signal from the source node and retransmits to the destination node instantly. The received signal Y_{RD} at the destination can be written as (5)

$$Y_{RD} = \sqrt{P_R} h_{RD} (\beta_r Y_{SR}) + n_{RD} \tag{5}$$

where β_r is the amplifying factor as in (6).

$$\beta_r = \sqrt{\frac{1}{|h_{SR}|^2 P_S + \sigma^2}} \tag{6}$$

where h_{SR} is the fading coefficient between the source node and the relay node, P_S is the signal transmission power, and σ^2 is the noise power for the $S \rightarrow R$ channel.

At the destination, the signals received from the source node and the relay node are combined using Maximal Ratio Combining (MRC). Therefore, based on (4) and (5), the combined signal can be expressed as (7).

$$Y^{UAF} = \alpha_1 Y_{SD} + \alpha_2 Y_{RD} \tag{7}$$

where

$$\begin{cases} \alpha_1 = \dfrac{\sqrt{P_S h_{SD}^*}}{\sigma^2} \\ \alpha_2 = \dfrac{\sqrt{\frac{P_S P_R}{P_S |h_{SR}|^2 + \sigma^2}} h_{SR}^* h_{RD}^*}{(\frac{P_R |h_{RD}|^2}{P_S |h_{SR}|^2 + \sigma^2} + 1)\sigma^2} \end{cases}$$

According to (7), the total received signal-to-noise ratio (SNR) can be further written as (8).

$$\gamma^{UAF} = \gamma_{sd} + \gamma^*$$

where

$$\begin{cases} \gamma_{sd} = \dfrac{P_S |h_{SD}|^2}{\sigma^2} \\ \gamma^* = \dfrac{\gamma_{sr} \gamma_{rd}}{1 + \gamma_{sr} + \gamma_{rd}} \\ \gamma_{sr} = \dfrac{P_S |h_{SR}|^2}{\sigma^2} \\ \gamma_{rd} = \dfrac{P_R |h_{RD}|^2}{\sigma^2} \end{cases}$$

Obviously, the total SNR in (8) can be upper-bounded as $\gamma_u^{UAF} = \gamma_{sd} + \gamma^{'}$, where $\gamma^{'} = min\{\gamma_{sr},\ \gamma_{rd}\}$. Since $S \rightarrow D$ channel is Nakagami fading, the PDF of γ_{sd} can be written as (9)[18].

$$p_{\gamma_{sd}}(\gamma) = \frac{m_0^{m_0} \gamma^{m_0 - 1}}{\bar{\gamma_{sd}}^{m_0} \Gamma(m_0)} e^{-\frac{m_0 \gamma}{\bar{\gamma_{sd}}}} \tag{9}$$

where m_0 is the Nakagami-m fading parameter of $S \rightarrow D$ channel, $\Gamma(\cdot)$ is the gamma function, and $\bar{\gamma_{sd}} = E(\gamma_{sd})$.

As for the PDF of $\gamma^{'}$, we first compute its cumulative density function (CDF) $F_{\gamma'}(\gamma)$ in (10) with the assumption that γ_{sr} and γ_{rd} are independently distributed [19].

$$F_{\gamma'}(\gamma) = 1 - [1 - F_{\gamma_{sr}}][1 - F_{\gamma_{rd}}] \tag{10}$$

where $F_{\gamma_{sr}}$ and $F_{\gamma_{rd}}$ are CDFs of γ_{sr} and γ_{rd}, respectively.

Therefore, through the first-order differentiation of its CDF, the PDF of $\gamma^{'}$ can be written as (11).

$$p_{\gamma'}(\gamma) = \frac{(\frac{m_{\gamma_{sr}}}{\bar{\gamma_{sr}}})^{m_{\gamma_{sr}}} \gamma^{m_{\gamma_{sr}} - 1} e^{-\frac{m_{\gamma_{sr}} \gamma}{\bar{\gamma_{sr}}}} \Gamma(m_{\gamma_{rd}}, \frac{m_{\gamma_{rd}}}{\bar{\gamma_{rd}}} \gamma)}{\Gamma(m_{\gamma_{rd}}) \Gamma(m_{\gamma_{sr}})} + \frac{(\frac{m_{\gamma_{rd}}}{\bar{\gamma_{rd}}})^{m_{\gamma_{rd}}} \gamma^{m_{\gamma_{rd}} - 1} e^{-\frac{m_{\gamma_{rd}} \gamma}{\bar{\gamma_{rd}}}} \Gamma(m_{\gamma_{sr}}, \frac{m_{\gamma_{sr}}}{\bar{\gamma_{sr}}} \gamma)}{\Gamma(m_{\gamma_{rd}}) \Gamma(m_{\gamma_{sr}})} \tag{11}$$

where $\Gamma(\alpha, x)$ is the incomplete gamma function [20], $\bar{\gamma_{sr}} = E(\gamma_{sr})$, $\bar{\gamma_{rd}} = E(\gamma_{rd})$, $m_{\gamma_{sr}}$ and $m_{\gamma_{rd}}$ are the Nakagami-m

fading parameters of $S \rightarrow R$ channel and $R \rightarrow D$ channel, respectively.

Furthermore, the BER expression for the UAF scheme is derived for BPSK modulation. Through averaging over conditional BER $P_e^{UAF}(Y|\gamma_{sd},\gamma^{'}) = Q(\sqrt{\gamma_u^{UAF}})$,where $Q(x)$ is the Q-function which is defined as $Q(x) = \frac{1}{\sqrt{2pi}}\int_x^\infty e^{-\frac{u^2}{2}}du$, the average BER can be written as a two-folded integral in (12).

$$P_e(Y)^{UAF} = \int_0^\infty \int_0^\infty P_e^{AF}(Y|\gamma_{sd},\gamma^{'})p_{\gamma_{sd}}(\gamma_a)p_{\gamma'}(\gamma_b)d\gamma_a d\gamma_b \tag{12}$$

Note that, (12) can be adopted for other modulation methods, including M-PSK, even for nonconstant modulus transmissions like M-ary amplitude modulation (M-AM) and M-QAM.

B. UDF Mode

In UDF mode, as shown in Fig. 5(b), the relay first demodulates the received signal. If successful, it re-modulates the data and forwards it to the destination. Otherwise, the relay cannot help the source node for the current cooperation round. Specifically, if the instantaneous SNR is larger than a specified threshold, it helps the source to forward this packet; otherwise, it does not help to forward but drops this packet.

Furthermore, the received signals at the relay node and the destination terminal are the same as in the UAF mode as shown in (3) and (4). And the received signal Y_{RD}^{UDF} at the destination can be written as (13), where X_R is the transmitted signal by the relay node, and γ_{th} is a specified threshold for SNR.

$$Y_{RD}^{DF} = \begin{cases} \sqrt{P_R}h_{RD}X_R + n_{RD}, & if\ \gamma_{sr} \geq \gamma_{th} \\ 0, & otherwise \end{cases} \tag{13}$$

Thus, in UDF mode, the received signal at the destination can be expressed as in (14).

$$Y^{UDF} = \begin{cases} \alpha_1^{UDF}Y_{SD} + \alpha_2^{UDF}Y_{RD}^{UDF}, & if\ \gamma_{sr} \geq \gamma_{th} \\ 0, & otherwise \end{cases} \tag{14}$$

where

$$\begin{cases} \alpha_1^{UDF} = \dfrac{\sqrt{P_S}h_{SR}^*}{\sigma^2} \\ \alpha_2^{UDF} = \dfrac{\sqrt{P_R}h_{RD}^*}{\sigma^2} \end{cases}$$

Therefore, the output SNR at the destination γ^{UDF} can be written as (15).

$$\gamma^{UDF} = \begin{cases} \gamma_{sd} + \gamma_{rd}, & if\ \gamma_{sr} \geq \gamma_{th} \\ \gamma_{sd}, & otherwise \end{cases} \tag{15}$$

Considering that γ^{DF} is a Nakagami random variable, we can now derive the BER expression for the UDF scheme with BPSK modulation. Through averaging over conditional BER $P_e^{UDF}(Y|\gamma^{sr},\gamma^{rd},\gamma^{sd}) = Q(\sqrt{\gamma^{DF}})$, the average BER can be written as a integral given by (16).

$$P_e(Y)^{UDF} = \int_0^\infty P_e^{UDF}(Y|\gamma^{sr},\gamma^{rd},\gamma^{sd})p_{\gamma_{DF}}(\gamma)d\gamma \tag{16}$$

where $p_{\gamma_{DF}}$ is the PDF of γ_{DF}.

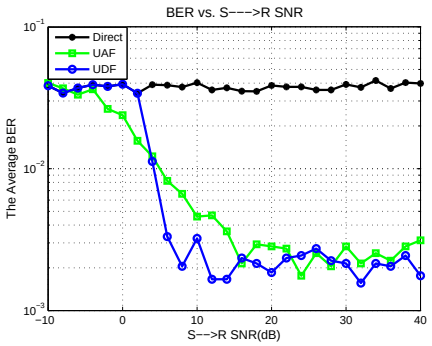

Fig. 6. Performance Comparison of UAF, UDF and Direct Transmission

C. Direct Transmission

For the direct transmission, firstly we can write the conditional BER in a Q function form as $P_e^{Direct}(Y|\gamma_{sd}) \approx Q(\sqrt{\gamma_{sd}})$, where γ_{sd} is the instantaneous SNR for the $S \rightarrow D$ link and it is a Nakagami random variable. Then, based on an integral, we can get average BER as in (17).

$$P_e^{Direct} = \int_0^\infty P_e^{Direct}(Y|\gamma_{sd})p_{\gamma_{DF}}(\gamma)d\gamma \tag{17}$$

D. Performance Comparison of AF, DF and Direct Transmission Schemes

As shown in Fig. 6, the BER performances of transmission cooperative diversity (UAF, UDF) and direct transmission schemes are compared, where $\gamma_{sd} = 2dB$ and $\gamma_{rd} = 4dB$. It shows that, if the SNR condition in the SR link is relatively poor, the UAF outperforms the UDF. On the contrary, if the SNR condition in the SR link is good enough, UDF outperforms UAF. The important observation obtained from Fig. 6 is that the transmission performance is different according to the SNR conditions. Therefore we proposed a hybrid forwarding scheme which selects between UAF, UDF and direct transmission schemes to achieve optimal BER performance.

E. Hybrid Forwarding Scheme

The proposed hybrid forwarding algorithm is described as follows: The relay node measures γ_{sr} firstly via the assistance of channel reciprocity principle. If γ_{sr} is larger than a specified SNR threshold, the relay node selects UDF; otherwise, it selects UAF. The relay node informs the destination node on the type of forwarding scheme used, by transmitting a one-bit message. The destination terminal performs appropriate MRC combining.

V. Numerical Results

Our simulation system contains two major components: acoustic field module and communication channel module.

We use Bellhop Gaussian beam tracing program [15] for the acoustic field module, which computes the sound transmission loss and multipath propagation parameters (including path numbers, delay spread, and amplitudes for each macro-path). Specific sound speed profiles are required for our simulations.

Here the sound speed profiles include: Taiwan straits sound-speed profile (water depth is 62 meters) in 1998 which was conducted and analyzed in [21], the Santa Barbara sound-speed profile described in [22] (Water depth is maintained at 250m), and the Munk sound profile [23], which is a 5000 meter deep water sound speed file. The source emits 40 kHz sound with launching angles within a 100 degree range facing the receiver.

The output from the acoustic field module is then fed into the communication channel module. It evaluates the underwater acoustic channel based on the proposed methods in Section III. Here we assume that the noise level is 10^{-5} W and transmission power is set to guarantee the average SNR for the home channel be 2 dB. We run each simulation 500 times and use the average value for each statistic.

In Fig. 7(a)-(d), it is seen that the BER varies with relay locations near the surface. Here the source, the relay, and the destination are all located underwater at 10 meters. The destination is located 2000 m away from the source, and the relay locates at $100 \sim 1900$ m along the line from the source to the destination. In Fig. 7(a), the sound speed, observed in May in Taiwan Strait, China, varies from 1527 to 1528 m/s, which is nearly constant. In Fig. 7(b), the sound speed, sampled in January in Taiwan Strait, China, varies from 1510 to $1515m/s$, and it increases positively. In Fig. 7(c), the sound speed observed under the Santa Barbara sound-speed profile varies from 1500 to $1487m/s$, and it follows a negative gradient. Fig. 7(d) shows the BER performance under the Munk sound profile as in Fig. 1(d). Although simulations are taken under different sound speed profiles, it shows similar trends on the variations of the BER in terms of the locations of the relay node. Compared to the direct transmission, UDF and UAF have better performance in most cases. Note that the performance improvement has the breathing effect. It means that the cooperative transmission can improve performance only when the relays are at certain locations. According to the simulation results, the breathing effect is more severe in shallow water scenario than that in deep water scenario. This breathing effect is caused by the directional transmission of acoustic signals, and the bouncing of signals from the surface and bottom. Furthermore, it is obvious that when the relay node is close to the source node, UDF outperforms UAF. When the relay node is near the destination, the performance of UDF is nearly equal to the performance of direct transmission. The reason is that, in UDF, the relay node will refuse to cooperate when it finds the channel from the source node to the relay node is bad. It also shows that the UAF protocol sometimes has better and sometimes has worse performance than direct transmission, and the performance depends on the location of the relay node.

As shown in Fig. 8, for the case where nodes are located near the sea floor and far from the sea surface (about 4900 m), the performance of direct transmission is poor and the relay can improve the performance with both UAF and UDF. Similar to Fig. 7, when the relay is near to the source node, UDF outperforms UAF; otherwise, UAF performs better than UDF. Besides, because terminals at different locations have different Amplitude−Delay Profiles caused by multipath propagations,

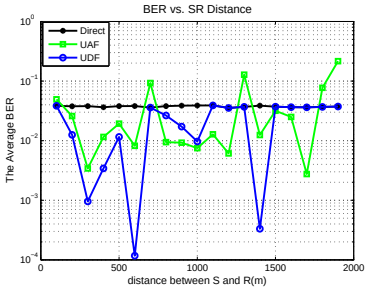

(a) Constant Sound Speed

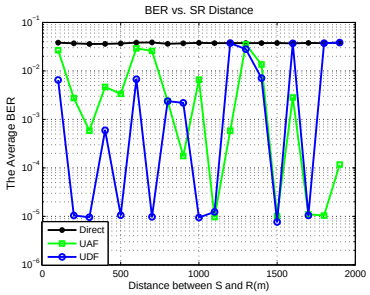

(b) Sound Speed with Positive Gradient

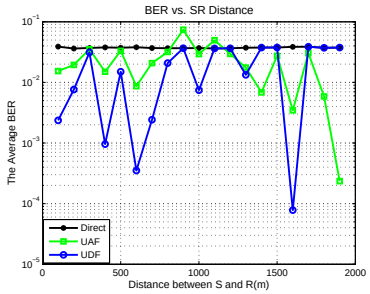

(c) Sound Speed with Negative Gradient

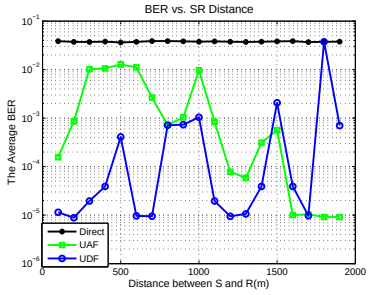

(d) Sound Speed in Deepsea

Fig. 7. BER vs. SR ranges

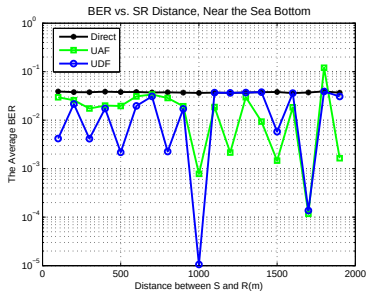

Fig. 8. BER vs. SR ranges, Near the Sea Bottom

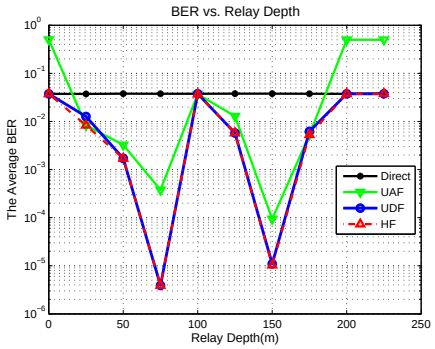

Fig. 9. BER vs. Relay Depths

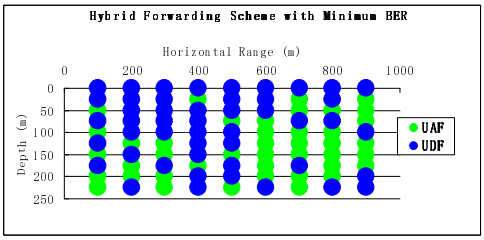

Fig. 10. Hybrid Forwarding Scheme with Minimum BER

the performance improvement through cooperative transmission has the breathing effect. It means that BER performance can be further improved through choosing the proper location for the relay node.

Fig. 9 shows that relay depth impacts BER performance. In this scenario, the source node is located underwater at 100 meters. The destination node is located on the sea surface. Their horizontal range is 1000 meters. The relay is located at the perpendicular bisector of the horizontal connecting line between the source and the destination nodes, which guarantee $z_1 = z_2 = 500$ meters. By changing the depth of the relay node, the best performance is achieved when the relay is 75m and 150m deep. This may be because the directional transmission of acoustic signals, and the bouncing of signals from the surface and bottom, make signals received from multipath propagation at a such special location specially enhanced.

Fig. 10 shows how our proposed Hybrid Forwarding Scheme works when the relay node is located at different horizontal ranges from the source. It is assumed that the source node is located underwater at 100m deep with the coordinates $(0, 100)$, and the destination node is on the sea surface which is 1000m away from the source node with the coordinates $(1000, 0)$. Based on this result, we can provide guidance for the relay node to select proper forwarding schemes to minimize BER according to its position in the system.

VI. Conclusion

In this paper, we investigate the application of cooperation diversity in UANs to improve communication reliability. We first proposed asynchronous transmission cooperative diversity for Underwater Acoustic Networks which can be implemented in presence of large and variable propagation delays and analyzed its performance in terms of Bit Error Rate with two basic forwarding schemes, Underwater Amplify-and-Forward and Underwater Decode-and-Forward. Our study shows that, when the channel condition in the source to the relay link is good, UDF performs better than UAF; when the channel condition in the source-to-destination link is not good, UAF outperforms UDF but not remarkably. The simulation results also show that the multipath effect of acoustic signal causes the breathing effect. Based on these analysis, we further proposed a hybrid forwarding scheme, in which the relay node adaptively chooses the best scheme among UAF, UDF and no relaying for given instantaneous SNR conditions. Through our simulation work, we find that the sound speed distribution of the area, sea depth, source depth, receiver depth and distance from the source, and related media parameters, have influence on performance of cooperative transmission. To summarise, for a specific network topology, the relay node should adopt proper forwarding scheme according to its location. In addition, considering the performance improvement through cooperation transmission has the breathing effect, network topology should be designed in an optimal way.

Our future research will extend the development of cooperation with more than one relay, which is a more realistic scenario. Besides, energy issue will be taken into consideration.

References

[1] J. Kong, J.-H. Cui, D. Wu, and M. Gerla, *Building Under-Water Ad-hoc Networks and Sensor Networks for Large Scale Real-time Aquatic Applications*, IEEE Milcom 2005, Atlantic, NJ, USA. October 17–21, 2005.

[2] I. F. Akyildiz, D. Pompili, and T. Melodia, *Underwater Acoustic Sensor Networks: Research Challenges*, Elsevier Journal of Ad Hoc Networks, Vol. 3, No. 3, May 2005. pp. 257-279.

[3] A. Stefanov and M. Stojanovic, *Clustered Multihop Transmission in Underwater Acoustic Ad-Hoc Networks*, in Proc. IEEE International Conference on Communication Systems (ICCS) 2010, Singapore. November 2010.

[4] C. Carbonelli, S.-H. Chen, and U. Mitra, *Error propagation analysis for underwater cooperative multi-hop communications*, Ad Hoc Networks, Vol. 7, No. 4, 2009. pp.759 - 769.

[5] C. Carbonelli and U. Mitra, *Cooperative multihop communication for underwater acoustic networks*, in Proceedings of the 1st ACM international workshop on Underwater networks, 2006. pp.97-100.

[6] M. Vajapeyam, U. Mitra, J. Preisig, and M. Stojanovic, *Distributed Space-Time Cooperative Schemes for Underwater Acoustic Communications*, in Proc. OCEANS 2006 - Asia Pacific, 2006. pp. 1-8.

[7] J.W. Han, H.J. Ju, K.M. Kim, *A Study on the Cooperative Diversity Technique with Amplify and Forward for Underwater Wireless Communication*, OCEANS 2008 - MTS/IEEE Kobe Techno-Ocean, Apr. 8-11, 2008. pp.1-3.

[8] Z. Han, Y. L. Sun, and H. Shi, *Cooperative Transmission for Underwater Acoustic Communications*, in Proc. IEEE International Conference on Communications (ICC '08), Beijing, China, 2008. pp. 2028-2032.

[9] H.J. Yang, F.Y. Ren, C. Lin,B. Liu, *Energy efficient cooperation in underwater sensor networks* , International Workshop on Quality of Service (IWQoS) 2010. pp.1-9.

[10] X. Geng and A. Zielinski, *An eigenpath Underwater Acoustic Communication Channel Model*, in Proc. Of MTS/IEEE OCEANS'95. 1995.

[11] C.B. Niese, R. Luten, *Statistical Simulation of Acoustic Communication in Turbulent Shallow Water*, IEEE Journal of Oceanic Engineering, Vol.25, No.4, 2000. pp.523-532.

[12] M.C. Domingo, R. Luten, *Overview of Channel Models for Underwater Wireless Communication Networks*, Physical Communication, Vol.1, Iss. 3, Sep. 2008. pp.163-182.

[13] B. Borowski, *Characterization of a very shallow water acoustic communication channel*, MTS/IEEE Biloxi - Marine Technology for Our Future: Global and Local Challenges, OCEANS 2009. pp.1-10.

[14] A. Zielinski, Y.-H. Yoon, L. Wu, *Performance analysis of digital acoustic communication in a shallow water channel*, IEEE Journal of Oceanic Engineering 20 (1995). pp.293-299.
[15] Available at ONR Ocean Acoustics Library, *http://oalib.hlsresearch.com/*.
[16] R. J. Urick, *Principles of underwater sound*, 3rd ed., McGraw-Hill, Inc. 1983.
[17] Y.X. Li, G.L. Liang, G.P. Zha, J. Fu, *The Application of LDPC Code in Underwater Acoustic Wireless Communications*, 5th International Conference on Wireless Communications, Networking and Mobile Computing, 2009 (WiCom '09), Sept.24-26, 2009. pp.1-3.
[18] M. K. Simon and M.-S. Alouini, *Digital Communication over Fading Channels: A Unified Approach to Performance Analysis*, New York, NY: Wiley. 2000.
[19] S. Ikki and M. H. Ahmed, *The Application of LDPC Code in Underwater Acoustic Wireless Communications*, IEEE Comm. Letters, Vol. 11, No. 4, Apr. 2007. pp.334-336.
[20] M. Nakagami, *The m-Distribution - A General Formula of Intensity Distribution of Rapid Fading*, in W. C. Hoffman (ed.): Statistical Methods in Radio Wave Propagation, Pergamon Press: New York, 1960. pp. 3-36.
[21] D.S. Chen, *Distributive features of sound velocity in middle and northern Taiwan Strait in February and March, 1998*, Journal of Oceanography in Taiwan Straits, Vol.19, No.3, Sep. 2000. pp.288-292.
[22] L.Y. Oey, C. Winant, E. Dever, W.R. Johnson, D.P. Wang, *A Model of the Near-Surface Circulation of the Santa Barbara Channel: Comparison with Observations and Dynamical Interpretations*, Journal of Physical Oceanography. Boston: Vol. 34, Iss. 1, Jan 2004. pp.23-40.
[23] D. Lucani, M. Medard and M. Stojanovic, *On the Relationship Between Transmission Power and Capacity of an Underwater Acoustic Communication Channel*, in Proc. IEEE Oceans'08 Conference, Kobe, Japan, 2008. April 2008.
[24] W. H. Munk, *Sound channel in an exponentially stratified ocean with applications to SOFAR*, Journal of the Acoustical Society America, 55(1974). pp.220–226